Research Article ISSN Online: 2783-4859 **Computational Mathematics and Computer Modeling with Applications**

Received 10 May 2023
Accepted 30 June 2023

DOI: 10.52547/CMCMA.1.2.104
AMS Subject Classification: 90C34; 76W05

Numerical solution for solving magnetohydrodynamic (MHD) flow of nanofluid by least squares support vector regression

Aida Pakniyat[a]

This paper introduces a new numerical solution based on the least squares support vector machine (LS-SVR) for solving nonlinear ordinary differential equations of high dimensionality. We apply the quasilinearization method to linearize the magnetohydrodynamic (MHD) flow of nanofluid around a stretching cylinder, thereby transforming it into a linear problem. We then utilize LS-SVR with fractional Hermite functions as basis functions to solve this problem over a semi-infinite interval. Our numerical results confirm the effectiveness of this approach.

Keywords: Cylinder, Spectral methods; Least squares support vector machine; Magnetohydrodynamic (MHD); Nonlinear ODE; fractional Hermite functions; Semi-infinite.

1. Introduction

We can define nanofluids simply as fluids that are capable of thermal transfer. Nanofluids have attracted the attention of many scientists in recent years due to the significant increase in thermal properties. The particle size used in nanofluids is from 1 *nm* to 100 *nm*. Nanofluids can improve heat transfer compared to pure liquids [61]. There are numerous publications on nanofluids' characteristics as transfer rates, greater viscosity, and higher thermal conductivity. A differential equation is used to understand the nanofluids problem. Khan et al [21] studied the boundary layer flow of a nanofluid past a stretching sheet. Parand et al. applied the Hermite pseudospectral method for solving the (MHD) flow [50]. Hayat et al. discussed [18] the flow of viscous nanofluid due to a rotating disk. Reddy et al. [55] analyzed the (MHD) boundary layer slip flow of a Maxwell nanofluid. In 2017, Ibrahim examined the (MHD) boundary layer stagnation point flow and heat transfer of a nanofluid [20].

There are various problems in unbounded domains. One of these methods is the spectral methods. Spectral methods have expanded rapidly over the past three decades. These methods have been widely used in various branches of science, such as fluid mechanics, quantum mechanics, physics, and chemistry [4, 12, 43]. At present, as with finite difference and finite element methods, they are powerful tools for solving the numerical differential equations [38, 47, 48]. Extraordinary features of spectral methods are high accuracy and infinite convergence. The main idea of these methods stems from the Fourier analysis [7, 11]. Spectral methods can be used to solve problems in semi-infinite domains. Guo et al. [13] proposed a method for semi-infinite intervals.

Researchers [41, 51] presented an approach that is based on the mapping of bases in semi-infinite domains. The use of mappings $x = \phi(\xi)$, $\phi : (-\infty, +\infty) \to [0, +\infty)$ is important problem. By placing $\phi(\xi)$ instead of x, the problem in the infinite intervals becomes a problem in the semi-infinite domains [42]. There is another approach for solving such problems which is based on rational approximations. In reference, [52] have applied spectral methods as a rational for this method. In addition, they have studied fractional approximations on unbounded domains [19, 22, 62]. Researchers have investigated the use of fractional orthogonal polynomials of order n and obtained the convergence of polynomials order [10, 46]. For example, for solving the Lane-Emden equation is used the operation matrix of fractional derivative Chebyshev polynomials is [39].

[a] *Department of Computer and Data Sciences, Faculty of Mathematical Sciences, Shahid Beheshti University, Tehran, Iran. Email: a_pakniyat@sbu.ac.ir.*
* *Correspondence to: A. Pakniyat*

Another approach is named domain truncation [7] and then is used for semi-infinite intervals $[0, x_{max}]$,where $x_{max}$is large enough to be selected. The researchers studied this approach to solve nonlinear different equations [40, 44]. When the domain truncation approach is used for infinite and semi-infinite intervals, As the x_{max} increases, the accuracy of the infinite order increases, the only way to do this is to increase the number of series sentences. Boyd [8] offers solutions for this method.

Machine learning methods can also be used to solve differential equations [26, 35], and one of these methods is the least squares support vector machine (LS-SVM) [34]. The support vector machine has gained massive popularity in recent years. The reason is their robust classification performance-even in high-dimensional spaces. The goal of the support vector machine algorithm is to obtain a hyperplane in n-dimensional space with a maximum margin. The n-the number of features that distinctly classify the data points [58, 59, 60]. Another advantage of the support vector machine is convergent, which must be global minima because it is a convex optimization problem [14]. Data points are classified based on n features [28, 29, 31, 58]. This type of learning system is used to both categorize and estimate the data fitness function. References have been able to use different bases in this method to solve differential equations in infinite and semi-infinite ranges [15, 49]. Mehrkanoon et al. [27] are using LS-SVM for solving the ordinary differential equation. The least squares regression method (LS-SVR) is another method for solving differential equations. We propose a solution for this problem based on LS-SVR with fractional Hermite functions.

The rest of this paper is organized as follows: in section 2, we consider the mathematical model to solve the nanofluids problem. In section 3, our method is described. We show the results of numerical experiments in section 4. Finally, a conclusion is presented in section 5

2. Mathematical Model

We consider the boundary layer flow of an electrically conducting nanofluid along with an impermeable stretching cylinder. In general, to model the (MHD) flow of the nanofluid, double stratification and thermal radiation effects are considered. In this section, we will focus on Hayat et al's discussion of the (MHD) flow of the nanofluid, which considers an impermeable stretching cylinder. [17] (Fig.1):

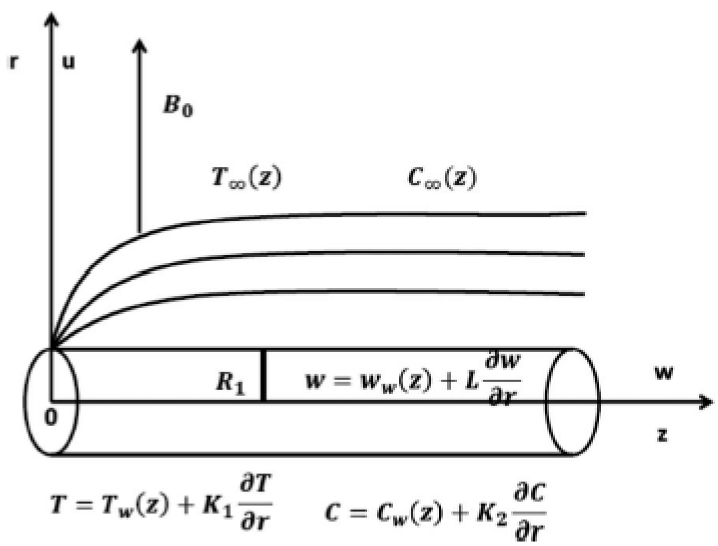

Figure 1. Physical model of the problem

For incompressible fluids, the law of conservation of mass is as follows:

$$\frac{\partial(ru)}{\partial r} + \frac{\partial(rw)}{\partial z} = 0, \tag{1}$$

A system's linear momentum is conserved according to the law of conservation of momentum. According to Newton's second law, this law is as follows:

$$u\frac{\partial w}{\partial r} + w\frac{\partial w}{\partial z} = \nu\left(\frac{\partial^2 w}{\partial r^2} + \frac{1}{r}\frac{\partial w}{\partial r}\right) - \frac{\sigma B_0^2}{\rho}w, \tag{2}$$

The momentum equation involves three types of forces. In this problem, the left-hand term represents inertial force, the right-hand term represents surface force, and the second term represents body force. According to the law of conservation of energy, the total energy in a system is conserved. As a result, this law is derived from the first law of thermodynamics, which states

$$u\frac{\partial T}{\partial r}+w\frac{\partial T}{\partial z}=\alpha\left(\frac{\partial^2 T}{\partial r^2}+\frac{1}{r}\frac{\partial T}{\partial r}\right)+\tau\left(D_B\frac{\partial C}{\partial r}\frac{\partial T}{\partial r}+\frac{D_T}{T_\infty}\left(\frac{\partial T}{\partial r}\right)^2\right)$$
$$+\frac{16}{3}\frac{\sigma^* T_\infty^3}{(\rho C)_f k^*}\left(\frac{\partial^2 T}{\partial r^2}+\frac{1}{r}\frac{\partial T}{\partial r}\right), \tag{3}$$

On the left side, there are terms representing the internal energy, while on the right side, there are terms representing the heat flux (diffusion). On the left side, there are terms reflecting Brownian motion and thermophoretic phenomena, while on the right side, there are terms representing thermal radiation

$$u\frac{\partial C}{\partial r}+w\frac{\partial C}{\partial z}=D_B\left(\frac{\partial^2 C}{\partial r^2}+\frac{1}{r}\frac{\partial C}{\partial r}\right)+D_T\left(\frac{\partial^2 T}{\partial r^2}+\frac{1}{r}\frac{\partial T}{\partial r}\right), \tag{4}$$

Accordingly, the boundary conditions to the magnetohydrodynamic flow of nanofluid are

$$\begin{aligned}
&w=w_w(z)+L\frac{\partial w}{\partial r},\quad u=0, T=T_w(z)+K_1\frac{\partial T}{\partial r},\ C=C_w(z)+K_2\frac{\partial C}{\partial r}\quad \text{at } r=R_1,\\
&w\to 0,\ T\to T_\infty(z),\ C\to C_\infty(z)\quad \text{as } r\to\infty,\\
&w_w(z)=\frac{\mathrm{U}_0 z}{l},\ T_w(z)=T_0+a\left(\frac{z}{l}\right),\ C_w(z)=C_0+b\left(\frac{z}{l}\right),\ T_\infty(z)=T_0+d\left(\frac{z}{l}\right),\\
&C_\infty(z)=C_0+e\left(\frac{z}{l}\right),\ \alpha=\frac{k}{(\rho C_p)_f},\ \tau=\frac{(\rho C_p)_p}{(\rho C_p)_f},\ \upsilon=\frac{-}{\rho_f}.
\end{aligned} \tag{5}$$

Here, u and w are the velocity components along the radial and axial directions, In Table1 lists the variables.

Table 1. The nomenclature of chemical compounds for model [17]

u, v	Velocity components	$L, K_1$and K_2	Velocity,Thermal and Concentration slip factors
C	Concentration	T	Temperature
υ	Kinematic viscosity	σ	Electrical conductivity
ρ	Density	α	Thermal diffusivity
D_B	Brownian diffusion coefficient	D_T	Thermophoresis diffusion coefficient
$(\rho C_p)_f$	Heat capacity of fluid	$(\rho C_p)_p$	Heat capacity of nanopaticle
ρ_f	Density	k	Thermal concentration
k^*	Mean absorption coefficient	$w_w(z)$	Stretching velocity
U_0	Reference velocity	l	Reference length
$T_w(z)$	Temperature over the surface	$T_\infty(z)$	Temperature for away from the surface
T_0	Reference temperature	$C_w(z)$	Concentration over the surface
$C_\infty(z)$	Ambient concentration	C_0	Reference concentration
a, b, d and e	Dimensional constants		

After applying the transformation shown below, Equation 1 is satisfied

$$\begin{aligned}
\eta=\sqrt{\tfrac{U_0}{\nu l}}\left(\tfrac{r^2-R_1^2}{2R_1}\right), w=\tfrac{U_0 z}{l}f'(\eta),\\
u=-\sqrt{\tfrac{\upsilon U_0}{l}}\tfrac{R_1^2}{r}f(\eta),\ \theta(\eta)=\tfrac{T-T_\infty}{T_w-T_\infty},\ \phi(\eta)=\tfrac{C-C_\infty}{C_w-C_0}.
\end{aligned} \tag{6}$$

By using Equations (2- 5) is identically satisfied and boundary conditions, the (MHD) flow of nanofluid becomes [17]

$$(1+2\gamma\eta)f''' + 2\gamma f'' + ff'' - f'^2 - M^2 f' = 0, \tag{7}$$

$$(1+2\gamma\eta)(1+\frac{4}{3}R)\theta'' + 2\gamma(1+\frac{4}{3}R)\theta' + \Pr(f\theta' - f'\theta - Sf') + (1+2\gamma\eta)\Pr Nb\theta'\phi' \\ +(1+2\gamma\eta)\Pr Nt\theta^2 = 0, \tag{8}$$

$$(1+2\gamma\eta)\phi'' + 2\gamma\phi' + \mathrm{Le}(f\phi' - f'\phi - Pf') + \frac{Nt}{Nb}(1+2\gamma\eta)\theta'' + 2\gamma\frac{Nt}{Nb}\theta' = 0, \tag{9}$$

$$f'(0) = 1 + \mathrm{A}f''(0),\ f(0) = 0,\ \theta(0) = 1 - \mathrm{S} + \mathrm{B}`'(0),\ \text{Œ}(0) = 1 - \mathrm{P} + \mathrm{B}_1\text{Œ}'(0), \\ f'(\infty) = 0,\ \theta(\infty) = 0,\ \phi(\infty) = 0. \tag{10}$$

In which γ is the curvature parameter, M is the magnetic parameter, R is the radiation parameter, Nb is the Brownian motion parameter, Nt is the thermophoresis parameter, Pris the Prandtl number, Le is the Lewis number, S is the thermal stratification parameter, P is the solutal stratification parameter, A is the velocity slip parameter, B is the thermal slip parameter, and $\mathrm{B}_1$is the solutal slip parameter [17], This parameter has the following values

$$\begin{aligned} &\gamma = \left(\frac{\nu l}{\mathrm{U}_0 R_1^2}\right)^2, \qquad M = \sqrt{\tfrac{\sigma l}{\rho \mathrm{U}_0}}\mathrm{B}_0, \qquad R = \frac{4\sigma^* T_\infty}{k^* k}, \\ &Nb = \tfrac{(\rho C_p)_p D_B (C_w - C_0)}{(\rho C_p)_f \nu}, \\ &Nt = \tfrac{(\rho C_p)_p D_T (T_w - T_0)}{(\rho C_p)_f \nu T_\infty}, \\ &Pr = \frac{\mu (C_p)_f}{k}, \qquad Le = \tfrac{\nu}{D_B}, \qquad S = \frac{d}{a}, \\ &P = \frac{e}{b}, \qquad A = L\sqrt{\tfrac{\mathrm{U}_0}{\nu l}}, \qquad \mathrm{B} = K_1\sqrt{\frac{\mathrm{U}_0}{\nu l}}, \\ &B_1 = K_2\sqrt{\tfrac{\mathrm{U}_0}{\nu l}}. \end{aligned} \tag{11}$$

In 2002, Andresson by using the exact analytical solution for the slip-flow of a Newtonian fluid past problem [3]. Mahmoud applied the fourth-order Runge-Kutta method to solve visco-elastic fluid [24]. Mahmoud et al. [25] presented the Chebyshev spectral methods for MHD flow and heat transfer of a micropolar fluid over a stretching surface with heat generation and slip velocity. Parand et al. [53] applied the spectral method to solve the visco-flow problem. The homotopy analysis method for the solution of Equation (7-9) is employed to obtain by Hayat et. al [17]. Daniel et. al examined the solution to this problem by entropy analysis [9].

3. Methodology

The objective of this section is to demonstrate the application of the proposed method in solving a problem related to nanofluids. By presenting the results of our solution and analyzing its effectiveness, we establish the potential of our method in solving similar problems in this field of study.

3.1. Hermite Functions

In this section, we apply the properties of the Hermite functions. First, we introduce the Hermite functions and explain why Usage of Hermite polynomials to solve differential equations at infinite distances is generally not suitable. To solve this problem, we use the collocation method based on Hermite functions. Unlike the Hermite polynomials, the Hermite functions are well-behaved due to their decay property. . The Hermite functions are defined as [45, 57]

$$\widetilde{H}_n = \frac{1}{\sqrt{2^n n!}} e^{\frac{-x^2}{2}} H_n(x),\ n \geq 0, x \in \mathbb{R}, \tag{12}$$

where, $\left\{\widetilde{H}_n\right\}$ is an orthogonal system in complete in $L^2(\mathbb{R})$, inner product of the space $L^2(\mathbb{R})$

$$\int_{-\infty}^{+\infty} \widetilde{H}_n(x)\widetilde{H}_m(x)dx = \sqrt{\pi}\delta_{nm}, \tag{13}$$

which, $n \geq 1$, δ_{nm} is the Kronecker delta function. One of the essential features of Hermite functions is the recurrence relationship of three-term

$$\widetilde{H}_{n+1}(x) = x\sqrt{\frac{2}{n+1}}\widetilde{H}_n - \sqrt{\frac{n}{n+1}}\widetilde{H}_{n-1}(x), \ n \geq 1,$$
$$\widetilde{H}_0(x) = e^{-x^2/2}, \widetilde{H}_1(x) = \sqrt{2}xe^{-x^2/2}, \tag{14}$$

The following equation can be obtained using the above formula and the Hermite polynomial recurrent relation [57]

$$\widetilde{H'}_n(x) = \sqrt{2n}\widetilde{H}_{n-1}(x) - x\widetilde{H}_n(x) = \sqrt{\frac{n}{2}}\widetilde{H}_{n-1}(x) - \sqrt{\frac{n+1}{2}}\widetilde{H}_{n+1}(x), \tag{15}$$

and the following is also an orthogonal relationship for deriving Hermit functions [57]

$$\int_{-\infty}^{+\infty} \widetilde{H'}_n(x)\widetilde{H'}_m(x)dx = \begin{cases} -\frac{\sqrt{n\pi(n-1)}}{2}, & m = n-2, \\ (n+\frac{1}{2})\sqrt{\pi}, & m = n, \\ --\frac{\sqrt{\pi(n+1)(n+2)}}{2}, & m = n+2, \\ 0, & Otherwise. \end{cases} \tag{16}$$

The Hermite polynomials are defined as the function of the weight function $w(x) = e^{-x^2}$at the domains $(-\infty, +\infty)$

$$\widetilde{P}_N = \left\{u : u = e^{-x^2/2}v, \ \forall v \in P_N\right\}, \tag{17}$$

where P_N is the set of all Hermite polynomials of the degree at most N. We introduce the Guass quadrature associated with the Hermite functions approach. Let $\{x_j\}_{j=0}^N$ are the Gauss-Hermite points and define the weights as follows :[57]

$$\widetilde{w}_j = \frac{\sqrt{\pi}}{(N+1)\widetilde{H}_N^2(x_j)}, \ 0 \leq j \leq N. \tag{18}$$

Then we have

$$\int_{-\infty}^{+\infty} p(x)dx = \sum_{j=0}^{N} p(x_j)\widetilde{w}_j, \ \forall p \in \tilde{P}_{2N+1}. \tag{19}$$

For solving the (MHD) flow of nanofluid problem, we use mapping because the Hermite functions are in infinite domains $(-\infty, +\infty)$. Here, the goal is to create a fractional Hermite function transferred to the semi-infinite domains. In general, the fractional form of Hermite functions is obtained by changing the variable of the form $x = t^\alpha$ $\alpha > 0$. The $F\widetilde{H}_n(t)$ a symbol is used to display it. Then we have

$$F\widetilde{H}_n(t) = \widetilde{H}_n(t^\alpha) \quad 0 \leq t < \infty, \tag{20}$$

or

$$F\widetilde{H}_n = \frac{1}{\sqrt{2^n n!}}e^{\frac{-(\frac{1}{k}\ln(t^\alpha))^2}{2}}H_n(\frac{1}{k}\ln(t^\alpha)), \quad n \geq 0, t \in [0, \infty), \tag{21}$$

which

$$F\widetilde{H}_0(t) = e^{\frac{-(\frac{1}{k}\ln(t^\alpha))^2}{2}}. \tag{22}$$

For the fractional order of the Hermite functions transferred to the semi-infinite domains, the recursive relationship will be as follows:

$$F\widetilde{H}_{n+1}(t) \quad = \tfrac{1}{k}\ln(t^\alpha)\sqrt{\tfrac{2}{n+1}}F\widetilde{H}_n(t) - \sqrt{\tfrac{n}{n+1}}F\widetilde{H}_{n-1}(t), \quad n \geq 1,$$
$$F\widetilde{H}_0(t) = e^{\frac{-(\frac{1}{k}\ln(t^\alpha))^2}{2}} \quad F\widetilde{H}_0(t) = \sqrt{2}\tfrac{1}{k}\ln(t^\alpha)e^{\frac{-(\frac{1}{k}\ln(t^\alpha))^2}{2}}. \tag{23}$$

The Hermite functions in the infinite domain are orthogonal to the weight function $w(x) = \frac{1}{x}$in the $[0, +\infty)$ interval. Therefore, the Hermite functions transferred from the fraction order in the semi-infinite domain are orthogonal to the weight function $w(t) = \frac{1}{t}$. The orthogonal relationship is as follows:

$$< F\widetilde{H}_n(t), F\widetilde{H}_m(t) >_{w(t)}= \sqrt{\pi}\delta_{nm}. \tag{24}$$

Fractional order transmitted Hermite functions $F\widetilde{H}_n(t)$ have n distinct real roots in an semi-infinite domain $[0, +\infty)$. Therefore, to obtain the zeros of the transferred Hermite functions, we have the inverse image fraction of the points of the space $\{x_j\}_{x_j=-\infty}^{x_j=+\infty}$as follows:

$$\Gamma = \{\phi^{-1}(p) \in D_E : -\infty < p < \infty\} = (0, +\infty). \tag{25}$$

We have a fraction for the transferred Hermite functions:

$$\tilde{t}_j = \phi^{-1}(x_j) = (e^{kx_j})^{\frac{1}{\alpha}}, \quad j = 0, 1, 2, \dots . \tag{26}$$

3.2. Support Vector Machine

We have training sets D, including the N points defined below

$$D = \{(x_i, y_i)|\ x_i \in \mathbb{R}^n, y_i \in \mathbb{R},\ n = 1\}_{i=1}^{N}, \tag{27}$$

$x_i \in \mathbb{R}^{\mathbf{n}}$ is the ith input data and $y_i \in \mathbb{R}$ is the ith output data. The goal is to find the separating hyperplane with the most considerable distance from the margin. Each hyperplane can be written as follows:

$$y(x) = w^T\varphi(x) + b, \tag{28}$$

where w is the weight vector, b is bias term and $\varphi(x)$ is a nonlinear function which is used to transform the nonlinear input data into a higher-dimensional space. Another method for solving these problems, the primal LS-SVR model as follows:[16, 23, 27, 33, 58] that it is an optimization problem

$$\begin{aligned} &\min_{w,b,e} \quad \frac{1}{2}w^T w + \frac{\lambda}{2}e^T e, \\ &\text{sbject to} \quad y_i = w^T\varphi(x_i) + b + e_i, \quad i = 1, \dots, N, \end{aligned} \tag{29}$$

where $\lambda \in \mathfrak{R}^+$. Instead of [29], we can easily use the dual model that obtains after the Lagrangian multipliers and conditions for optimal (KKT conditions) will be as follows [5, 23, 30, 33, 36, 37]

$$\begin{bmatrix} \mathrm{M} + \frac{1}{\lambda}I_N & 1_N \\ 1_N^T & 0 \end{bmatrix} \begin{bmatrix} \alpha \\ b \end{bmatrix} = \begin{bmatrix} y \\ 0 \end{bmatrix}, \tag{30}$$

here, M is kernel matrix that calculated by $\mathrm{M}_{\mathrm{i,j}} =< \varphi(x), \varphi(y) >= k(x, y)$, Section 3.3 briefly describes it. $1_N = [1, \dots, 1]^T \in \mathbb{R}^{\mathbb{N}}, \alpha = [\alpha_1, \dots, \alpha_N]^T, y = [y_1, \dots, y_N]^T$. I_N is an $N \times N$ identity matrix. Applying KKT conditions for the primal model and its derivative from e, w and equalizing it to zero, it will eliminate these .Because of this feature, in infinite-dimensional, kernel trick is used to solve the problem. The corresponding dual model illustration is $y(x) = \sum_{i=1}^{N} \alpha_i k(x, y) + b$ [30]. When dimensional is high, solving the problem with the dual model is more satisfied. The kernel functions plays a role in the higher dimensional space. We have shown that the following differential operators, which are used to solve the problem in the next section that they are the derivative of the kernel function. [5, 27, 33]

$$\nabla_n^m \equiv \frac{\partial^{n+m}}{\partial x^n \partial^m y}, \tag{31}$$

$$[\varphi^{(n)}(x)].\varphi^{(m)}(y) = \nabla_n^m[\varphi(x), \varphi(y)] = \nabla_n^m[k(x, y)] = \frac{\partial^{n+m} k(x, y)}{\partial x^n \partial^m y}, \tag{32}$$

for instance, we have given here some example

$$\begin{aligned} &\nabla_1^0[k(x, y)] = \varphi^{(1)}(x).\varphi^{(0)}(y), \quad \nabla_0^1[k(x, y)] = \varphi^{(0)}(x).\varphi^{(1)}(y), \\ &\nabla_2^0[k(x, y)] = \varphi^{(2)}(x).\varphi^{(0)}(y), \quad \nabla_0^2[k(x, y)] = \varphi^{(0)}(x).\varphi^{(2)}(y), \\ &\nabla_3^0[k(x, y)] = \varphi^{(3)}(x).\varphi^{(0)}(y), \quad \nabla_0^3[k(x, y)] = \varphi^{(0)}(x).\varphi^{(3)}(y). \end{aligned} \tag{33}$$

Therefore, the proposed LS-SVR algorithm for solving differential equations is represented in 1.

Algorithm 1 The general LS-SVR algorithm for sloving the differential equation

1. Get values of boundary/ initial values and set parameter of LS-SVR (λ)
2. Perform differential equation
3. LS-SVR model
   (a) Input: ode differential equations (First, the non-linear equation becomes a linear equation)
   (b) Output: compute the weight vector
      i. for $i = 1$ to N do
      ii. The LS-SVR model can be given by $y(x) = \sum_{i=1}^{N} \alpha_i k(x, y) + b$
      iii. Set kernel function (fractional Hermite functions) and their parameters
      iv. end for
   (c) Train model with the LS-SVR model and then evaluate with this model

In Figure 2 represented simple computational steps of LS-SVR with inputs [1]. In Sections (3.2,3.3 and 3.5) deal with this issue in more detailed information.

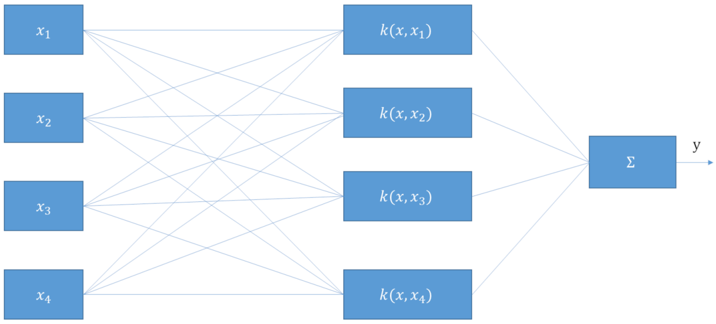

Figure 2. Mathematical model of LS-SVR for $n = 4$

In this figure, x_i, y showed inputs and output respectively, and $k(x, y)$ is kernel trick that in this paper, fractional Hermite functions have been selected.

3.3. Kernel Functions

The kernel matrix k is calculated $k(x, y) =< \varphi(x), \varphi(y) >$, x, y are n-dimensional inputs. φ is the map from n-dimensional to m-dimensional space. $< x, y >$ denotes the dot product. Kernel trick makes it possible to get the same results, even with every high degree polynomials, without actually having to add them. Support vector machines also work for non-linear problems by using the kernel trick. This method helps linear learning algorithm to learn a non-linear function which determines the decision boundary. The SVM kernel is a function that takes low dimensional input space and transforms it to a higher dimensional space. It is the ultimate benefit of non-linear separation problems. Our kernel functions in this paper are Hermite functions that are included Mercer's condition [30, 32, 63], then used instead of linear algorithms in high-dimensional problems. Here, employing Hermite functions becomes well-conditions and good performance and avoid over-fitting. The Mercer's conditions is as follow

$$\int\int_{\Omega} k(x, y)g(x)g(y)dxdy \geq 0, \quad \forall g \in L_2, \Omega \subseteq \Re. \tag{34}$$

If the kernel functions have the Mercer's conditions, the kernel used will be satisfied. So, it can represent the Hermite functions as follows: [2, 45, 57]

$$k(x, y) = \sum_{i=0}^{m} H_i(x)H_i(y), \tag{35}$$

where the Hermite functions H_n is orthogonal and positive definite kernel [30], we have elaborated the properties of Hermite functions in the Section (3.1) that the Mercer's theorem holds for the Hermite functions for vector spaces.

3.4. Quasilinearization Method

A compelling approximation technique for solving nonlinear differential equations is the quasilinearization method. (QLM). This procedure is repeated until a rapid, and often uniform convergence is achieved. Bellman and Kalaba introduced the Newton-Raphson method for solving one or a set of ordinary and partial differential equations [6]. In this method, the nonlinear differential equation becomes a sequence of linear differential equations, and the solution of this sequence of linear differential equations is uniformly converged to the solution of the desired nonlinear differential equation. This method has been used by many researchers [45, 54, 56]. This method requires an initial guess, which is usually selected based on the initial conditions and the physical and mathematical properties of the problem [40, 45]. To know how it works, imagine that we have a simple differential equation as [45]

$$y''(x) = f(y), \qquad y(0) = y(b) = 0, \tag{36}$$

$y_0(x)$ is an initial approximation of the solution. Consider the $\{y_r\}$ sequence as follows:

$$y''_{r+1} = f(y_r) + (y_{r+1} - y_r)f_y(y_r), \quad y_{r+1}(0) = y_{r+1}(b) = 0. \tag{37}$$

Nonlinear differential equations with the following ordinary derivatives are available in the intervals $[0, b]$

$$L^{(n)}y(x) = f(y(x), y^{(1)}(x), ..., y^{(n-1)}(x), x), \tag{38}$$

with n boundary condition

$$\begin{aligned} &g_k(y(0), y^{(1)}(0), ..., y^{(n-1)}(0)) = 0, \quad k = 1, ..., l, \\ &g_k(y(b), y^{(1)}(b), ..., y^{(n-1)}(b)) = 0, \quad k = l+1, ..., n. \end{aligned} \tag{39}$$

L is a regular linear differential operator of order n, and f , $g_1, g_2, ..., g_n$ are the nonlinear functions of $y(x)$ and be its derivatives. The value of b can be infinite. $y_{r+1}(x)$ is the solution to the following linear differential equation that is presented as the response to the nonlinear differential equation (38):

$$\begin{aligned} &L^n y_{r+1}(x) = f(y_r(x), y_r^{(1)}(x), ..., y_r^{(n-1)}(x), x) \\ &+\sum_{s=0}^{n-1}(y_{r+1}^{(s)}(x) - y_r^{(s)}(x))f_{y^{(s)}}(y_r(x), y_r^{(1)}(x), ..., y_r^{(n-1)}(x), x), \end{aligned} \tag{40}$$

where $y_r^{(0)}(x) = y_r(x)$ and linear boundary conditions

$$\begin{aligned} &\sum_{s=0}^{n-1}(y_{r+1}^{(s)}(0) - y_r^{(s)}(0))g_{ky^{(s)}}(y_r(0), y_r^{(1)}(0), ..., y_r^{(n-1)}(0), 0), \quad k = 1, ..., l, \\ &\sum_{s=0}^{n-1}(y_{r+1}^{(s)}(b) - y_r^{(s)}(b))g_{ky^{(s)}}(y_r(b), y_r^{(1)}(b), ..., y_r^{(n-1)}(b), b), \quad k = l, ..., n+1, \end{aligned} \tag{41}$$

where $f_{y^{(s)}}$ and $g_{ky^{(s)}}$ functions are derivatives of the following functions, respectively

$$\begin{aligned} &f(y_r(x), y_r^{(1)}(x), ..., y_r^{(n-1)}(x), x), \\ &g_k(y_r(x), y_r^{(1)}(x), ..., y_r^{(n-1)}(x), x). \end{aligned} \tag{42}$$

3.5. Application of the Method

For solving the (MHD) flow of nanofluid problem, we are used QLM and LS-SVR methods based on fractional Hermite functions. Using the QLM, the Equations (7-8) that non-linear equations make linear sequence equations. Accordingly, the solution of the equations (7-8) is the $(n+1)$ iterative approximation of the following linear differential equations.

$$\begin{aligned} \frac{d^3 f_{n+1}}{dJ^3} &= F(f''_n, f'_n, f_n, \eta) + (f_{n+1} - f_n)\frac{\partial F}{\partial f_n}(f''_n, f'_n, f_n, \eta) + (f'_{n+1} - f'_n)\frac{\partial F}{\partial f'_n}(f''_n, f'_n, f_n, \eta) \\ &+ (f''_{n+1} - f''_n)\frac{\partial F}{\partial f''_n}(f''_n, f'_n, f_n, \eta), \end{aligned} \tag{43}$$

$$\frac{d^2 \grave{}_{n+1}}{dJ^2} = \Theta(\theta'_n, \theta_n, \eta) + (\theta_{n+1} - \theta_n)\frac{\partial \Theta}{\partial \theta_n}(\theta'_n, \theta_n, \eta) + (\theta'_{n+1} - \theta'_n)\frac{\partial \Theta}{\partial \theta'_n}(\theta'_n, \theta_n, \eta), \tag{44}$$

we can be calculated with the boundary conditions (10). We consider the initial guesses (f_0, θ_0, ϕ_0)[17] for the QLM method, which satisfying in the boundary condition.

$$f_0(\eta) = \frac{1}{1+A}(1-\exp(-\beta\eta)), \quad \theta_0(\eta) = \frac{1-S}{1+B}\exp(-\kappa\eta), \quad \phi_0(\eta) = \frac{1-P}{1+B_1}\exp(-\varpi\eta), \tag{45}$$

and β, κ and ϖ are constants. In this paper, we have used the fractional Hermite roots in the interval $[0,+\infty)$ that are a set of training points, we have

$$y(x) = w^T\varphi(x) + b, \tag{46}$$

where, is the approximate solution for Equations (43-44-9) that w, b are the optimal values of model are obtained by solving the optimization problem. Firstly, we expand $f(\eta)$, $\theta(\eta)$ and Œ(ȷ) as follows:

$$\xi_N f(\eta) = \sum_{j=0}^{N-1} w1_j\widetilde{\varphi}_j(\eta), \quad \xi_N\theta(\eta) = \sum_{j=0}^{N-1} w2_j\widetilde{\varphi}_j(\eta), \quad \xi_N\phi(\eta) = \sum_{j=0}^{N-1} w3_j\widetilde{\varphi}_j(\eta), \tag{47}$$

where $w1_j$, $w2_j$ and $w3_j$, $j = 0\ldots N-1$ are unknown coefficients, φ_j, $j = 0\ldots N-1$ are transformed fractional Hermite functions and the N are collocation points. In Section (3.1), we defined an orthogonal projection based on the transformed fractional Hermite functions. The $\xi_N : L^2(\Gamma) \to \widetilde{H}_N$ is a mapping in a way that for any $y \in L^2(\Gamma)$, the $L^2(\Gamma)$ is the orthogonal projection, will have

$$< \xi_N y - y, \phi >= 0, \quad \forall_\phi \in \widetilde{H}_N, \tag{48}$$

or equivalently,

$$\xi_N y(\eta) = \sum_{j=0}^{N-1} w_j\widetilde{H}_j(\eta). \tag{49}$$

Thus, we have

$$\widetilde{\xi}\psi_1(\eta) = f_0(\eta) + \xi_N f(\eta), \quad \widetilde{\xi}\psi_2(\eta) = \theta_0(\eta) + \xi_N\theta(\eta), \quad \widetilde{\xi}\psi_3(\eta) = \phi_0(\eta) + \xi_N\phi(\eta) \tag{50}$$

We can substitute $\widetilde{\xi}\psi_1(\eta)$, $\widetilde{\xi}\psi_2(\eta)$ and $\widetilde{\xi}\psi_3(\eta)$ into Equations (43,44,9) and we construct the residual functions by finding the solution of the following optimization problem

$$\begin{aligned} &\min_{w,b,e} \quad \frac{1}{2}w^Tw + \frac{\lambda}{2}e^Te, \\ &\text{subject to} \quad w^T\varphi^{(M)}(\eta_i) + \sum_{k=1}^{M-1} w^T r_k(\eta_i)\varphi^{(k)}(\eta_i) = e_i, \quad i = 2\ldots N, \\ &w^T\varphi(\eta_1) + b = p_0, \end{aligned} \tag{51}$$

here, $r_k(\eta)$ is a specified function and (M) represents a nonlinear ordinary differential equation of a given order. To further our analysis, we introduce residual functions $Res1(\eta)$, $Res2(\eta)$, and $Res3(\eta)$, which are defined by the following equations:

$$\begin{aligned} Res1(\eta) = &-\frac{d^3(\text{-}_1)_{n+1}}{d\jmath^3} + F((\psi_1'')_n, (\psi_1')_n, (\psi_1)_n, \eta) + ((\psi_1)_{n+1} - (\psi_1)_n)\frac{\partial F}{\partial(\psi_1)_n}((\psi_1'')_n, (\psi_1')_n, (\psi_1)_n, \eta) \\ &+((\psi_1')_{n+1} - (\psi_1')_n)\frac{\partial F}{\partial(\psi_1')_n}((\psi_1'')_n, (\psi_1')_n, (\psi_1)_n, \eta) + ((\psi_1'')_{n+1} - (\psi_1'')_n)\frac{\partial F}{\partial(\psi_1'')_n}((\psi_1'')_n, (\psi_1')_n, (\psi_1)_n, \eta), \end{aligned} \tag{52}$$

where

$$F((\psi_1'')_n, ((\psi_1')_n, (\psi_1)_n, \eta) = (1+2\gamma\eta)(\psi_1''')_n + 2\gamma(\psi_1'')_n + f(\psi_1'')_n - ((\psi_1')_n)^2 - M^2(\psi_1')_n, \tag{53}$$

by employing the roots of transformed Hermite functions at collocation points N, represented by η in Equation (7), we can utilize the QLM method to generate $n+1$ linear differential equations.

$$\begin{aligned} Res2(\eta) = &-\frac{d^2(\text{-}_2)_{n+1}}{d\jmath^2} + \Theta((\psi_2')_n, (\psi_2)_n, \eta) + ((\psi_2)_{n+1} - (\psi_2)_n)\frac{\partial\Theta}{\partial(\psi_2)_n}((\psi_2')_n, (\psi_2)_n, \eta) \\ &+(\theta'_{n+1} - \theta'_n)\frac{\partial\Theta}{\partial(\psi_2')_n}((\psi_2')_n, (\psi_2)_n, \eta), \end{aligned} \tag{54}$$

where

$$\Theta((\psi_2')_n,(\psi_2)_n,\eta)=(1+2\gamma\eta)(1+\frac{4}{3}R)(\psi_2'')_n+2\gamma(1+\frac{4}{3}R)(\psi_2')_n+\Pr((\psi_1)_n(\psi_2')_n-(\psi_1')_n(\psi_2)_n-S(\psi_1')_n)$$
$$+(1+2\gamma\eta)\Pr Nb(\psi_2')_n\psi_3'+(1+2\gamma\eta)\Pr Nt((\psi_2)_n)^2, \tag{55}$$

equation (54) provides $n+1$ linear equations that can be obtained using the QLM method. $Res2$ is formed by utilizing the roots of transformed Hermite functions.

$$Res3(\eta)=(1+2\gamma\eta)\psi_3''+2\gamma\psi_3'+\mathrm{Le}((\psi_1)_n\psi_3'-(\psi_1')_n\psi_3-P(\psi_1')_n)+\frac{Nt}{Nb}(1+2\gamma\eta)(\psi_2')_n+2\gamma\frac{Nt}{Nb}(\psi_2')_n. \tag{56}$$

The obtained placement f_{new} from Equation (52) is used to solve a set of equations in the QLM method by replacing it in Equations (54-56). The QLM method is utilized to obtain θ_{new}, which is then substituted in Equation (56). Finally, a quadratic programming problem is solved to find the unknown coefficients for all of these equations. In this paper, the dual model is used to solve the quadratic programming problem. Thus, we can re-write Equations (51) in the following form:

$$\begin{aligned}
&\min_{w,b,e}\ \frac{1}{2}w^Tw+\frac{\lambda}{2}e^Te,\\
&w_1^T\psi_1'''(\eta_i)+\sum_{k=1}^{3}Res1_k(\eta_i)=e_i,\quad i=2...N_1,\quad w_1^T\psi_1(\eta_1)+b_1=p_0,\\
&w_2^T\psi_2''(\eta_i)+\sum_{k=1}^{2}Res2_k(\eta_i)=e_i,\quad i=2...N_2,\quad w_2^T\psi_2(\eta_1)+b_2=q_0,\\
&w_3^T\psi_3''(\eta_i)+\sum_{k=1}^{2}Res3_k(\eta_i)=e_i,\quad i=2...N_3\quad w_3^T\psi_3(\eta_1)+b_3=u_0,
\end{aligned} \tag{57}$$

Here, $\psi_1,;\psi_2;$ and; ψ_3 represent the transformed fractional Hermite functions, and the parameter value $\lambda\in\Re^+$. By substituting Equations (57), the following dual form can be computed:

$$\min\quad \frac{1}{2}\alpha^TH\alpha-1^T\alpha, \tag{58}$$
$$\text{subject to}\quad \sum_{\mathrm{i}}\text{ffiyi}=0,\quad \text{ffi}\geq 0. \tag{59}$$

The Lagrangian of the optimization problem is constructed by substituting Equations (57) into the following function:

$$\mathcal{L}(w_1,\alpha_i,e_i)=\frac{1}{2}w_1^Tw_1+\frac{\lambda}{2}e^Te+\sum_{i=2}^{N_1}\alpha_i\left[w_1^T\psi_1'''(\eta_i)+\sum_{k=1}^{3}Res1_k(\eta_i)+p_0-e_i\right], \tag{60}$$
$$\mathcal{L}(w_2,\beta_i,\xi_i)=\frac{1}{2}w_2^Tw_2+\frac{\lambda}{2}\xi^T\xi+\sum_{i=2}^{N_2}\beta_i\left[w_2^T\psi_2''(\eta_i)+\sum_{k=1}^{2}Res2_k(\eta_i)+q_0-\xi_i\right], \tag{61}$$
$$\mathcal{L}(w_3,\gamma_i,\vartheta_i)=\frac{1}{2}w_3^Tw_3+\frac{\lambda}{2}\vartheta^T\vartheta+\sum_{i=2}^{N_3}\gamma_i\left[w_3^T\psi_3''(\eta_i)+\sum_{k=1}^{2}Res3_k(\eta_i)+u_0-\vartheta_i\right], \tag{62}$$

The weight vectors (unknown coefficients) are denoted by $w_1,;w_2;$and; w_3, and the Lagrange multipliers are represented by $\alpha_i,;\beta_i,;$and; $\gamma_i\quad i=2...N$, where $N=[N_1,N_2,N_3]$. Furthermore, slack variables such as $e,;\xi;and;\vartheta$ are also included. The Karush-Kuhn-Tucker (KKT) conditions are employed for Equations (60-62) to compute the partial derivatives, resulting in the following equations:

$$\begin{aligned}
&\frac{\partial\mathcal{L}}{\partial w_1}=0\Rightarrow w_1=\sum_{i=2}^{N_1}\alpha_i\left[\psi_1'''(\eta_i)+\sum_{k=1}^{3}Res1_k(\eta_i)\right],\\
&\frac{\partial\mathcal{L}}{\partial\alpha_i}=0\Rightarrow w_1^T\psi_1'''(\eta_i)+\sum_{k=1}^{3}Res1_k(\eta_i)+p_0-e_i,\quad i=2,..N,\\
&\frac{\partial\mathcal{L}}{\partial e_i}=0\Rightarrow \alpha_i+Ce_i=0,\quad i=2,..N.
\end{aligned} \tag{63}$$

In the following, we apply the kernel trick, eliminate w_1; and; e from Equation (63), and write the solution using Mercer's condition. The resulting equation can be expressed as follows:

$$\begin{pmatrix} 0 & 1_N^T \\ 1_N & \mathbf{K}+\frac{1}{\lambda} \end{pmatrix}^{-1} \begin{pmatrix} b \\ \alpha \end{pmatrix} = \begin{pmatrix} y \\ p_0 \end{pmatrix}, \tag{64}$$

where

$$\begin{aligned} \frac{\partial \mathcal{L}}{\partial w_2} &= 0 \Rightarrow w_2 = \sum_{i=2}^{N_2} \beta_i \left[\psi_2''(\eta_i) + \sum_{k=1}^{2} Res2_k(\eta_i) \right], \\ \frac{\partial \mathcal{L}}{\partial \beta_i} &= 0 \Rightarrow w_2^T \psi_2''(\eta_i) + \sum_{k=1}^{2} Res2_k(\eta_i) + q_0 - \xi_i, \quad i = 2, ..N, \\ \frac{\partial \mathcal{L}}{\partial \xi_i} &= 0 \Rightarrow \beta_i + C\xi_i = 0, \quad i = 2, ..N, \end{aligned} \tag{65}$$

In the same way, w_2 and ξ eliminating and applying the kernel trick.

$$\begin{aligned} \frac{\partial \mathcal{L}}{\partial w_3} &= 0 \Rightarrow w_3 = \sum_{i=2}^{N_3} \gamma_i \left[\psi_3''(\eta_i) + \sum_{k=1}^{2} Res3_k(\eta_i) \right], \\ \frac{\partial \mathcal{L}}{\partial \gamma_i} &= 0 \Rightarrow w_3^T \psi_3''(\eta_i) + \sum_{k=1}^{2} Res3_k(\eta_i) + u_0 - \vartheta_i, \quad i = 2, ..N, \\ \frac{\partial \mathcal{L}}{\partial \vartheta_i} &= 0 \Rightarrow \gamma_i + C\vartheta_i = 0, \quad i = 2, ..N. \end{aligned} \tag{66}$$

We eliminated w_3; and; ϑ by utilizing the kernel trick with Mercer's condition in the dual form. To obtain the solution using LS-SVR, we applied the fractional Hermite function as the kernel trick, and its corresponding dual form representation is presented below.

$$\hat{y}_1 = \sum_{i=2}^{N_1} \alpha_i \left(\left[\nabla_3^0 K\right](\eta_i, \eta) - \sum_{k=1}^{3} Res1_k(\eta_j) \left[\nabla_{3-k}^0 K\right](\eta_i, \eta) \right), \tag{67}$$

$$\hat{y}_2 = \sum_{i=2}^{N_2} \beta_i \left(\left[\nabla_2^0 K\right](\eta_i, \eta) - \sum_{k=1}^{2} Res2_k(\eta_j) \left[\nabla_{2-k}^0 K\right](\eta_i, \eta) \right), \tag{68}$$

$$\hat{y}_3 = \sum_{i=2}^{N_3} \gamma_i \left(\left[\nabla_2^0 K\right](\eta_i, \eta) - \sum_{k=1}^{2} Res3_k(\eta_j) \left[\nabla_{2-k}^0 K\right](\eta_i, \eta) \right). \tag{69}$$

The dual form can be used to solve $Res1(\eta)$ with fractional Hermite functions as basis functions and obtain the w_1 coefficients by employing N_1 collocation points. The number of interpolated nodes in $Res2(\eta)$ and $Res3(\eta)$ is denoted by N_2 and N_3 respectively. The solution to $Res1(\eta)$ provides $\hat{y}_1$, which is then applied to Equations (68,69) to obtain w_2 and w_3 coefficients. These unknown coefficients are simultaneously obtained by solving the equations through the substitution of the previously acquired w_1. Algorithm 2 summarizes this method.

Algorithm 2 Estimation of the proposed LS-SVM method for solving (MHD) equation

Input: Initial values, number of collocation points, number of repetitions, regularization parameter λ, pick nominal values for this model
output: $\hat{y}$

1. Using fractional Hermite functions as bias function
2. Transformed fractional Hermite functions in interval $[0, +\infty)$
   for $i = 1$ to N do
   for $i = 1$ to $nlgm$ do
   - Applying QLM method for the nonlinear differential equation becomes a sequence of linear differential equations
     (a) Imposing the boundary conditions
     (b) The initial guesses which satisfying in the boundary condition

   end for
   (a) The approximate solution $y(x) = w^T \varphi(x) + b$
      i. Select the kernel function k and set its parameters (using Mercer's condition)
      ii. Compute the kernel matrix Ω
   (b) Construct the residual functions of the set of linear differential equations by finding the solution of the following optimization problem
      i. Obtain model parameter (α) by Lagrange multipliers and applying KKT conditions
      ii. Using the dual model for solving the quadratic programming, $y(x) = \sum_{i=1}^{N} \alpha_i k(x, y) + b$
      iii. Estimate $\hat{y}$

   end for

4. Numerical results

This section discusses the results of our study on using the LS-SVR method with fractional Hermite functions to solve the (MHD) flow of nanofluid problem. In our implementation, we employed fractional Hermite functions with $\alpha = 1/2$ as basis functions.

We present numerical results for various parameters including the velocity, temperature, and concentration to confirm the convergence of the LS-SVR method. Figure 3 illustrates the effect of the velocity slip parameter A on $f'(\eta)$, where an increase in A leads to a reduction in $f'(\eta)$. Moreover, Figure 4 shows the impact of parameters S and B on the temperature profile $\theta(\eta)$.

Additionally, in Figure 5, we display the graphs of the approximation of $\phi(\eta)$ for different values of parameters B and P. Finally, Tables (2-6) present the numerical solutions obtained. Our results demonstrate the accuracy and reliability of our proposed approach in solving the (MHD) flow of nanofluid problem effectively.

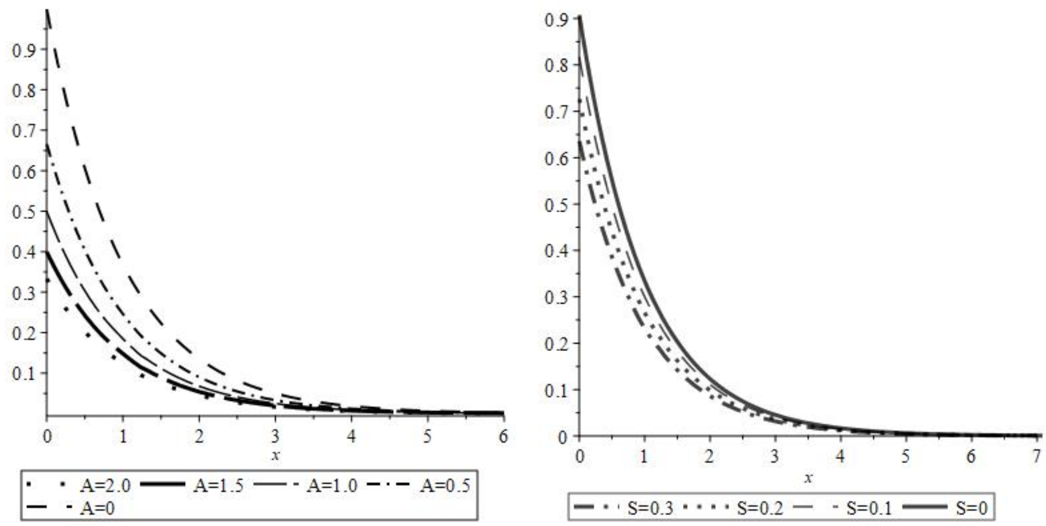

Figure 3. $f'(\eta)$ for several values of A (The left side), $\theta(\eta)$ for several values of S (The right side)

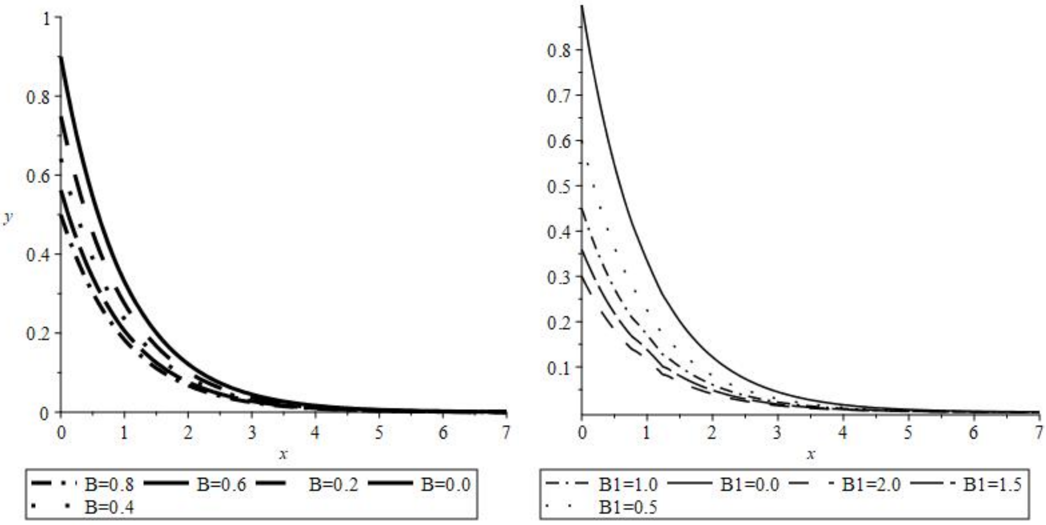

Figure 4. $\theta(\eta)$ for several values of B (The left side), $\phi(\eta)$ for several values of B (The right side)

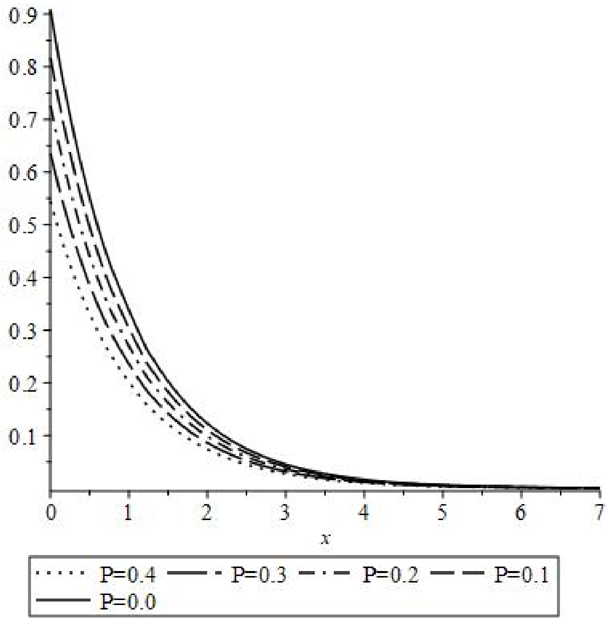

Figure 5. $\phi(\eta)$ for several values of P

Table 2. Comparison of $f'(0)$ for various A between Andersson, Mahmoud, Mahmoud and Waheed, Hayat and the present method when $\gamma = 0,\ M = 0$

$f'(0)$						
A	Andersson [3]	Mahmoud [24]	Mahmoud and Waheed [25]	Hayat [17]	Present results	β
0	1.0	1.0	1.0	1.0	1.0	1.0
0.1	0.9128	0.91279	0.91279	0.91279	0.9127900	1.004069
0.2	0.8447	0.84473	0.84472	0.84473	0.8447341	1.013681
0.5	0.7044	0.70440	0.70440	0.70440	0.7044000	1.0566
1.0	0.5698	0.56984	0.56982	0.56984	0.5698450	1.13969
2.0	0.4320	0.43204	0.43199	0.43204	0.4320433	1.29613
5.0	0.2758	0.27579	0.27579	0.27580	0.2756833	1.6541
10.0	0.1876	0.18758	0.18759	0.18781	0.1878182	2.066
20.0	0.1242	0.12423	0.12420	0.12456	0.1245638	2.61584

Table 3. Comparison of $f''(0)$ for various A between Andersson, Mahmoud, Mahmoud and Waheed, Hayat and the present method when $\gamma = 0,\ M = 0$

$f''(0)$						
A	Andersson [3]	Mahmoud [24]	Mahmud and Waheed [25]	Hayat [17]	Present results	β
0	1.0	1.0	1.0	1.0	1.0	1.0
0.1	0.8721	0.87208	0.87209	0.872082	0.872081	0.9794334
0.2	0.7764	0.77637	0.77639	0.776377	0.776377	0.965222
0.5	0.5912	0.59119	0.59121	0.591195	0.591199	0.9417
1.0	0.4302	0.43016	0.43018	0.430159	0430158	0.927533
2.0	0.2840	0.28398	0.28400	0.283978	0.283975	0.922999
5.0	0.1448	0.14484	0.14481	0.144841	0.1448452	0.93224
10.0	0.0812	0.08124	0.08123	0.081242	0.8124252	0.94534
20.0	0.0438	0.04378	0.04381	0.043772	0.4377242	0.95876

Table 4. Comparison of $f''(0)$ for various A, γ and M between Hayat and the present method

$-f''(0)$					
γ	M	A	Hayat [17]	Present results	β
0.0	0.2	0.1	0.9511	0.9511110	1.02285
0.5			1.1007	1.100740	1.10037
1.0			1.2337	1.233792	1.164977
0.1	0.0		0.9021	0.9021587	0.99618
	0.5		1.0889	1.088928	1.09445
	1.0		1.2391	1.239164	1.16751
	0.2	0.0	1.1352	1.135226	1.06547
		0.5	0.6554	0.6532681	0.9899
		1.0	0.4724	0.4724254	0.72088

Table 5. The comparison of $(1+\frac{4R}{3})\theta'(0)$ for different values for the present method and Hayat

												$(1+\frac{4R}{3})\theta'(0)$			
γ	M	R	Pr	S	Nb	Nt	P	Le	A	B	B_1	Hayat [17]	Present method	β	κ
0.0	0.2	0.1	1.4	0.1	0.1	0.1	0.1	1.9	0.1	0.1	0.1	0.9808	0.98084	1	1.0578
0.2												1.0343	1.0348	1	1.116
0.4												1.0855	1.0855	1	1.1707
0.1	0.0											1.0372	1.0376	1	1.119
	0.2											1.0079	1.0079	1	1.08699
	0.4											0.9823	0.98297	1	1.06010
	0.2	0.0										0.9478	0.94745	1	1.15799
		0.2										1.0631	1.0633	1	1.026010
		0.4										1.1603	1.1608	1	1.28199
		0.1	1.0									0.8422	0.84287	1	0.909
			1.5									1.0442	1.0447	1	1.014
			2.0									1.2034	1.2036	1	1.29799
			1.4	0.0								1.0426	1.0428	1	1.0122
				0.2								0.9732	0.97340	1	1.181
				0.4								0.9035	0.90387	1	1.4622
				0.1	0.2							0.9684	0.96804	1	1.044
					0.4							0.8937	0.89387	1	0.964
					0.6							0.8243	0.82432	1	0.889
					0.1	0.0						1.0325	1.0323	1	1.67
						0.2						0.9839	0.98349	1	1.591
						0.4						0.9392	0.93898	1	1.519
						0.1	0.0					1.0056	1.0057	1	1.627
							0.2					1.0103	1.0138	1	1.64
							0.4					1.0151	1.0150	1	1.642
							0.1	1.5				1.0121	1.0125	1	1.638
								2.0				1.0068	1.0064	1	1.628
								2.5				1.0031	1.0033	1	1.623
								1.9	0.0			1.0576	1.0571	1	1.71
									0.2			0.9675	0.96742	1	1.565
									0.4			0.9037	0.90375	1	1.462
									0.1	0.0		1.1072	1.1070	1	1.628
										0.2		0.9248	0.92421	1	1.631
										0.4		0.7927	0.79275	1	1.6322
										0.1	0.0	1.0041	1.0045	1	1.625
											0.2	1.0108	1.0107	1	1.635
											0.4	1.0149	1.0144	1	1.641

Table 6. The comparison of $\phi'(0)$ for different values for the present method and Hayat

												$\phi'(0)$				
γ	M	R	Pr	S	Nb	Nt	P	Le	A	B	B_1	Hayat [17]	Present method	β	κ	ϖ
0.0	0.2	0.1	1.4	0.1	0.1	0.1	0.1	1.9	0.1	0.1	0.1	0.7479	0.74945	1	1	0.916
0.2												0.8038	0.80345	1	1	0.982
0.4												0.8576	0.85909	1	1	1.05
0.1	0.0											0.8070	0.80754	1	1	0.987
	0.2											0.7760	0.77645	1	1	0.949
	0.4											0.7492	0.74921	1	1	0.9157
	0.2	0.0										0.7403	0.74037	1	1	0.9049
		0.2										0.8061	0.80615	1	1	0.9853
		0.4										0.8541	0.85418	1	1	1.044
		0.1	1.0									0.8618	0.86187	1	1	1.0534
			1.5									0.7568	0.75682	1	1	0.925
			2.0									0.66936	0.66934	1	1	0.81809
			1.4	0.0								0.7705	0.77056	1	1	0.9418
				0.2								0.7818	0.78185	1	1	0.9556
				0.4								0.7936	0.79363	1	1	0.97
				0.1	0.2							0.9994	0.99900	1	1	1.221
					0.4							1.1103	1.1103	1	1	1.357
					0.6							1.1466	1.1446	1	1	1.399
					0.1	0.0						1.1976	1.1976	1	1	1.4637
						0.1						0.7761	0.77613	1	1	0.9486
						0.2						0.3822	0.38225	1	1	0.4672
						0.1	0.0		0.0			0.8176	0.81764	1	1	0.8994
							0.2		0.2			0.7347	0.73476	1	1	1.0103
							0.4					0.6521	0.65214	1	1	1.1956
							0.1	1.5				0.5954	0.59547	1	1	0.7278
								2.0				0.8169	0.81695	1	1	0.9985
								2.5				1.0010	1.0010	1	1	1.2235
								1.9	0.0			0.8150	0.81507	1	1	0.9962
									0.2			0.7443	0.74431	1	1	0.90971
									0.4			0.6943	0.69431	1	1	0.8486
									0.1	0.0		0.7360	0.73603	1	1	0.8996
										0.2		0.8100	0.81000	1	1	0.99
										0.4		0.8636	0.86367	1	1	1.0556
										0.1	0.0	0.8886	0.88866	1	1	0.9874
											0.2	0.6891	0.68918	1	1	0.9189
											0.4	0.5627	0.56270	1	1	0.87531

5. Conclusions

In this paper, we introduced a numerical solution for solving nonlinear problems using LS-SVR. Our proposed algorithm consists of three key steps: selecting training points, quasilinearization, and utilizing fractional Hermite functions. First, we utilized Hermite roots to generate the necessary training data. Next, we employed the quasilinearization method to linearize the MHD flow problem. To improve the convergence of our solution via LS-SVR, we introduced fractional Hermite functions. Finally, we compared the results obtained using our proposed method with those obtained using other methods. Our findings demonstrate the effectiveness of this approach in solving nonlinear problems with high precision and efficiency.

References

1. R. Adnan, Z. Liang, X. Yuan, O. Kisi, M. Akhlaq, and B. Li. Comparison of LSSVR, M5RT, NF-GP, and NF-SC models for predictions of hourly wind speed and wind power based on cross-validation. *Energies*, 12(2):329–350, 2019.
2. A. A. Aghaei and K. Parand. Hyperparameter optimization of orthogonal functions in the numerical solution of differential equations. *arXiv e-prints*, page arXiv:2304.14088, 2023.
3. H. Andersson. Slip flow past a stretching surface. *Acta Mechanica*, 158:121–125, 2002.
4. F. Baharifard, K. Parand, and M. Rashidi. Novel solution for heat and mass transfer of a MHD micropolar fluid flow on a moving plate with suction and injection. *Engineering with Computers*, pages 1–18, 2020.
5. M. Baymani, O. Teymoori, and S. Ghasem. ϵ-least square support vector method for solving differential equations. *Am. J. Comput. Sci. Inf. Eng.*, 3(1):1–6, 2016.
6. R. Bellman, H. Kagiwada, and R. Kalaba. Orbit determination as a multipoint boundary-value problem and quasilinearization. *Proc. Nat. Acad. Sci.*, 48:1327–1329, 1962.
7. J. Boyd. *Chebyshev and Fourier Spectral Methods*. Dover Publications, 2000.
8. J. Boyd. Rational Chebyshev series for the Thomas–Fermi function: Endpoint singularities and spectral methods. *J. Comput. Appl. Math*, 244:90–101, 2013.
9. Y. Daniel, Z. Aziz, Z. Ismail, and F. Salah. Entropy analysis in electrical magnetohydrodynamic (MHD) flow of nanofluid with effects of thermal radiation, viscous dissipation, and chemical reaction. *Theor. Appl. Mech. Lett.*, 7:235–242, 2017.
10. M. Delkhosh and K. Parand. A new computational method based on fractional Lagrange functions to solve multi-term fractional differential equations. *Numerical Algorithms*, pages 1–38, 2021.
11. D. Funaro. *Polynomial approximation of differential equations*. Springer, Berlin, 1st edition, 1992.
12. C. Gheorghiu. *Spectral methods for differential problems*. Institute of Numerical Analysis, 2007.
13. B. Guo, J. Shen, and C. Xu. Spectral and pseudospectral approximations using Hermite functions: application to the Dirac equation. *Advances in Computational Mathematics*, 19:35–55, 2003.
14. Y. Guo, P. He, X. Wang, Y. Zheng, C. Liu, and X. Cai. Fast prediction with sparse multikernel LS-SVR using multiple relevant time series and its application in avionics system. *Mathematical Problems in Engineering*, pages 460514–460523, 2015.
15. A. Hadian-Rasanan, D. Rahmati, S. Gorgin, and K. Parand. A single layer fractional orthogonal neural network for solving various types of Lane–Emden equation. *New Astronomy*, 75:101307, 2020.
16. Z. Hajimohammadi and K. Parand. Numerical learning approximation of time-fractional sub diffusion model on a semi-infinite domain. *Chaos, Solitons & Fractals*, 142:110435, 2021.
17. T. Hayat, A. Nassem, M. Khan, M. Farooq, and A. Al-Saedi. Magnetohydrodynamic (MHD) flow of nanofluid with double stratification and slip conditions. *Physics and Chemistry of Liquids*, 56:189–208, 2018.
18. T. Hayata, M. Khana, M. Waqas, T. Yasmeen, and A. Alsaedib. Viscous dissipation effect in flow of magnetonanofluid with variable properties. *Journal of Molecular Liquids*, 222:47–54, 2016.
19. D. Hou and C. Xu. A fractional spectral method with applications to some singular problems. *Advances in Computational Mathematics*, 43(5):911–944, 2017.
20. W. Ibrahim. Magnetohydrodynamic (MHD) boundary layer stagnation point flow and heat transfer of a nanofluid past a stretching sheet with melting. *Propulsion and Power Research*, 6:214–222, 2017.
21. W. Khan and I. Pop. Boundary-layer flow of a nanofluid past a stretching sheet. *International Journal of Heat and Mass Transfer*, 53:2477–2483, 2010.
22. H. Khosravian-Arab, M. Dehghan, and M. Eslahchi. Fractional spectral and pseudo–spectral methods in unbounded domains: theory and applications. *Journal of Computational Physics*, 338:527–566, 2017.
23. Y. Lu, Q. Yin, H. Li, H. Sun, Y. Yang, and M. Hou. The LS-SVM algorithms for boundary value problems of high-order ordinary differential equations. *Adv. Differ. Equ.*, pages 1–22, 2019.
24. M. Mahmoud. Chemical reaction and variable viscosity effects on flow and mass transfer of a non-Newtonian visco-elastic fluid past a stretching surface embedded in a porous medium. *Meccanica*, 45:835–846, 2010.
25. M. Mahmoud and S. Waheed. Mhd flow and heat transfer of a micropolar fluid over a stretching surface with heat generation (absorption) and slip velocity. *J. Egypt. Math. Soc.*, 20:20–27, 2012.
26. H. D. Mazraeh, M. Kalantari, S. H. Tabasi, A. A. Aghaei, Z. Kalantari, and F. Fahim. Solving Fredholm integral equations of the second kind using an improved cuckoo optimization algorithm. *Global Analysis and Discrete Mathematics*, 7(1):33–52, 2023.
27. S. Mehrkanoon, T. Falck, and J. Suykens. Approximate solutions to ordinary differential equations using least squares support vector machines. *Neural Processing Letters*, 23(9):1356–1367, 2012.
28. F. Mirzaee, E. Solhi, and N. Samadyar. Moving least squares and spectral collocation method to approximate the solution of stochastic Volterra–Fredholm integral equations. *Applied Numerical Mathematics*, 161:275–285, 2021.
29. M. Moayeri, J. Rad, and K. Parand. Dynamical behavior of reaction–diffusion neural networks and their synchronization arising in modeling epileptic seizure: A numerical simulation study. *Computers & Mathematics with Applications*, 80(8):1887–1927, 2020.

30. V. Moghaddam and J. Hamidzadeh. New Hermite orthogonal polynomial kernel and combined kernels in support vector machine classifier. *Pattern Recognition*, 60:921–935, 2016.
31. S. Ozer, C. Chen, and H. Cirpan. A set of new Chebyshev kernel functions for support vector machine pattern classification. *Expert Systems with Applications*, 44(7):1435–1447, 2011.
32. S. Ozer, C. Chen, and H. Cirpan. A set of new Chebyshev kernel functions for support vector machine pattern classification. *Pattern Recognition*, 44(7):1435–1447, 2011.
33. K. Parand, A. Aghaei, M. Jani, and A. Ghodsi. A new approach to the numerical solution of Fredholm integral equations using least squares-support vector regression. *Mathematics and Computers in Simulation*, 180:114–128, 2021.
34. K. Parand, A. Aghaei, M. Jani, and A. Ghodsi. Parallel LS-SVM for the numerical simulation of fractional Volterra's population model. *Alexandria Engineering Journal*, 60(6):5637–5647, 2021.
35. K. Parand, A. Aghaei, S. Kiani, T. I. Zadeh, and Z. Khosravi. A neural network approach for solving nonlinear differential equations of Lane–Emden type. *Engineering with Computers*, pages 1–17, 2023.
36. K. Parand, A. A. Aghaei, M. Jani, and R. Sahleh. Learning with fractional orthogonal kernel classifiers in support vector machines: Theory, algorithms and applications. In *Springer Nature Singapore*, pages 199–224. Springer, Singapore, 2023.
37. K. Parand, F. Baharifard, A. A. Aghaei, and M. Jani. Learning with fractional orthogonal kernel classifiers in support vector machines: Theory, algorithms and applications. In *Springer*, pages 19–36. Singapore, 2023.
38. K. Parand, M. Dehghan, A. Rezaei, and S. Ghaderi. An approximation algorithm for the solution of the nonlinear Lane-Emden type equations arising in astrophysics using Hermite functions collocation method. *Computer Physics Communications*, 181(6):1096–1108, 2010.
39. K. Parand and M. Delkhosh. An effective numerical method for solving the nonlinear singular Lane-Emden type equations of various orders. *Jurnal Teknologi*, 79(1):25–36, 2017.
40. K. Parand and M. Delkhosh. Solving the nonlinear Schlomilch's integral equation arising in ionospheric problems. *Afr. Mat.*, 28(3):459–480, 2017.
41. K. Parand and M. Delkhosh. An accurate numerical method for solving unsteady isothermal flow of a gas through a semi-infinite porous medium. *Journal of Computational and Nonlinear Dynamics*, 13:011007–011015, 2018.
42. K. Parand and Z. Hajimohammadi. Using modified generalized Laguerre functions, QLM and collocation method for solving an Eyring-Powell problem. *Journal of the Brazilian Society of Mechanical Sciences and Engineering*, 40(4):1–9, 2018.
43. K. Parand, S. Hashemi-Shahraki, and M. Hemami. Unsteady flow of gas in a semi-infinite porous medium: a numerical investigation by using RBF-DQM. *Indian Journal of Physics*, pages 1–8, 2020.
44. K. Parand, Z. Kalantari, and M. Delkhosh. Quasilinearization-Lagrangian method to solve the HIV infection model of CD4 + T cells. *SeMA Journal*, 75(2):271–283, 2018.
45. K. Parand, Z. Kalantari, and M. Delkhosh. Solving the boundary layer flow of Eyring–Powell fluid problem via quasilinearization–collocation method based on Hermite functions. *The Indian National Academy of Engineering*, 3(1):11–19, 2018.
46. K. Parand, P. Mazaheri, H. Yousefi, and M. Delkhosh. Fractional order of rational Jacobi functions for solving the non-linear singular Thomas-Fermi equation. *The European Physical Journal Plus*, 132(77):1–13, 2017.
47. K. Parand and M. Razzaghi. Rational Chebyshev tau method for solving Volterra's population model. *Applied Mathematics and Computation*, 149:893–900, 2004.
48. K. Parand and M. Razzaghi. Rational Legendre approximation for solving some physical problems on semi-infinite intervals. *Physica Scripta*, 69:353, 2004.
49. K. Parand, M. Razzaghi, R. Sahleh, and M. Jani. Least squares support vector regression for solving Volterra integral equations. *Engineering with Computers*, pages 1–8, 2021.
50. K. Parand, A. Rezaei, and S. Ghaderi. An approximate solution of the MHD Falkner–Skan flow by Hermite functions pseudospectral method. *Communications in Nonlinear Science and Numerical Simulation*, 16:274–283, 2011.
51. K. Parand, A. Rezaei, and A. Taghavi. Lagrangian method for solving Lane-Emden type equation arising in astrophysics on semi-infinite domains. *Acta Astronautica*, 67(7-8):673–680, 2010.
52. K. Parand, A. Rezaei, and A. Taghavi. Numerical approximations for population growth model by rational Chebyshev and Hermite functions collocation approach: a comparison. *Mathematical Methods in the Applied Sciences*, 33:2076–2086, 2010.
53. J. Rad, K. Parand, and S. Kazem. A numerical investigation to viscous flow over nonlinearly stretching sheet with chemical reaction, heat transfer and magnetic field. *Int. J. Appl. Comput. Math.*, 3:919–935, 2017.
54. J. Rahimi, D. Ganji, M. Khaki, and K. Hosseinzadeh. Solution of the boundary layer flow of an Eyring-Powell non-Newtonian fluid over a linear stretching sheet by collocation method. *Alexandria Eng. J.*, 56(4):621–627, 2017.
55. P. Reddy, S. Suneeth, and N. Reddy. Numerical study of magnetohydrodynamics (MHD) boundary layer slip flow of a Maxwell nanofluid over an exponentially stretching surface with convective boundary condition. *Propulsion and Power*, 6:259–268, 2017.
56. A. Rezaei, F. Baharifard, and K. Parand. Quasilinearization–barycentric approach for numerical investigation of the boundary value fin problem. *Int J Comput Electr Autom Control Info Eng*, 5(2):194–201, 2011.
57. J. Shen, T. Tang, and L.-L. Wang. *Spectral methods: algorithms, analysis and applications*. Springer, New York, 2011.
58. J. Suykens, C. Alzate, and K. Pelckmans. Primal and dual model representations in kernel-based learning. *Statistics Surveys*, 4:148–183, 2010.
59. J. Suykens, T. V. Gestel, J. D. Brabanter, B. D. Moor, and J. Vandewalle. *Least squares support vector machines*. World Scientific Publishing Company, Singapore, 2002.
60. J. Suykens and J. Vandewalle. Least squares support vector machine classifiers. *Neural Processing Letters*, 9(3):293–300, 1999.
61. W. Yu and H. Xie. A review on Nanofluids: Preparation, stability mechanisms, and applications. *Journal of Nanomaterials*, pages 1–18, 2012.
62. M. Zayernouri and G. Karniadakis. Fractional spectral collocation method. *SIAM J. Sci. Comput.*, 36:A40–A62, 2014.
63. H. Zhang. Variable selection for support vector machine via smoothing spline ANOVA. *Statistica Sinica*, 16(2):659–674, 2006.

